Available online at www.sciencedirect.com
ScienceDirect
PERGAMON
Acta Astronautica 61 (2007) 806–815
ACTA ASTRONAUTICA
www.elsevier.com/locate/actaastro

1st ACT global trajectory optimisation competition: Results found at the Jet Propulsion Laboratory

Anastassios E. Petropoulos*, Theresa D. Kowalkowski, Matthew A. Vavrina, Daniel W. Parcher, Paul A. Finlayson, Gregory J. Whiffen, Jon A. Sims

Jet Propulsion Laboratory, California Institute of Technology, 4800 Oak Grove Dr., Pasadena, CA 91109-8099, USA

Available online 4 May 2007

Abstract

Results obtained at the Jet Propulsion Laboratory for the 1st ACT global trajectory optimisation competition are presented and the methods used to obtain them are described. The search for the globally optimal, low-thrust, gravity-assist trajectory for maximally deflecting an asteroid is performed in two steps. The first step involves a rough global search of the global search space, which has, however, been somewhat bounded based on prior mission-design experience, intuition, and energy arguments. A shape-based method is used to represent the low-thrust arcs, while the ballistic portions are searched almost exhaustively. The second step involves local optimisation of trajectories which stand out from the rough global search. The low-thrust optimisation problem is turned into a parameter optimisation problem by approximating the continuous thrusting as a series of impulsive manoeuvres. Of the many trajectories found, three optimal trajectories are reported and compared, including the one submitted for the competition. The best one employed a double-Venus, quadruple-Earth, Jupiter–Saturn–Jupiter gravity-assist sequence. The trajectory submitted for the competition used one less Venus flyby and one less Earth flyby.

Keywords: Trajectory design; Global optimisation; Low thrust; Electric propulsion; Gravity assist; Asteroid deflection

1. Introduction

The nature of the posed problem [1] made it clear from the outset that gravity assists should be used in maximising the objective function, and that some low-thrust manoeuvres would likely be necessary since the maximum launch hyperbolic excess velocity, v_∞, is barely sufficient to reach Venus. Thus, our search utilised techniques which encompassed both gravity assists and trajectory arcs of low thrust. The search for the globally optimal trajectory (it is likely that only one such trajectory exists) was conducted in two phases. First, an automated, rough global search, guided by mission design experience and intuition, was made over a very large part of the solution space, using a shape-based method for computing the low-thrust arcs [2,3]. Second, the most promising regions found in the rough search were examined more carefully with a local optimisation method [4], which transforms the low-thrust optimisation problem into a parameter optimisation problem. These two phases, which have been used in combination also in prior work [6], are described in Section 2. The results obtained and submitted for the competition are described in Section 3.

After the close of the competition, given the liberty of additional time for further investigations, several trajectories were found which improve on the highest

* Corresponding author. Tel.: +1 818 354 1509.
E-mail address: anastassios.e.petropoulos@jpl.nasa.gov (A.E. Petropoulos).

0094-5765/$ - see front matter © 2007 Published by Elsevier Ltd.
doi:10.1016/j.actaastro.2007.03.013

objective function value submitted to the competition. Two of these trajectories are reported in Section 4, which is followed by the concluding remarks.

2. General description of the method

2.1. Preliminary considerations

2.1.1. Is infinite velocity worthwhile?

The competition rules did not place a limit on the spacecraft propellant mass fraction: "dry mass can be considered zero." Therefore the propellant mass fraction can be arbitrarily large and in principle, be arbitrarily close to 1. This freedom combined with a maximum flight time of 30 years permits the possibility of consuming essentially all of the spacecraft mass as propellant. It requires 29.13 years to consume 1500 kg of propellant using the thruster defined in the competition. Using the symbols m_f for final spacecraft mass at impact, $\vec{U}_{rel}$ for the final spacecraft velocity relative to the asteroid, and $\vec{v}_{ast}$ for the asteroid's heliocentric velocity at impact, the objective function specified in the competition is

$$J = m_f |\vec{U}_{rel} \cdot \vec{v}_{ast}|. \tag{1}$$

Let us consider the objective function in the limit as the dry mass approaches zero. The mass at impact m_f will be approaching zero, but the velocity of impact will be approaching infinity in the classical case, or the speed of light in the relativistic case. A natural question is whether the final mass m_f approaches zero faster than the velocity becomes infinite, or whether the velocity approaches infinity faster than the mass approaches zero. If the latter is correct, then an infinite objective value J can be obtained. This question is obviously not relevant for real trajectory design, but is an interesting and instructive physics problem.

To answer this question, consider the ideal situation where the final velocity $\vec{U}_{rel}$ is exactly anti-parallel to the asteroid velocity $\vec{v}_{ast}$. Gravitational accelerations can be ignored as they are negligible when compared to the thrust acceleration for a spacecraft of infinitesimal mass. Further assume the ideal situation where all thrust acceleration is parallel to the spacecraft velocity to attain the maximum possible velocity. If the objective (1) cannot be made to be infinite in this case, then it can never be made infinite. The spacecraft mass at time t when thrusting continuously is given by

$$m(t) = m_o - \dot{m} \cdot t, \tag{2}$$

where m_0 is the initial spacecraft mass and $\dot{m}$ is the constant rate at which propellant mass is expended, i.e., the rate at which the spacecraft *loses* mass. In the classical case, the spacecraft acceleration at time t when thrusting with force T is

$$\dot{v}(t) = \frac{T}{m(t)}. \tag{3}$$

If (2) is substituted into (3) then integration will yield an expression for the velocity at time t, assuming T is constant:

$$v(t) = -\frac{T}{\dot{m}} \ln(m_o - \dot{m} \cdot t) + C, \tag{4}$$

where C is a constant of integration. Define x to be the quantity $m_o - \dot{m} \cdot t$. Then the limit we are interested in is

$$\lim_{x\to 0} J(x) \propto \lim_{x\to 0}[x \cdot v(x)] = \lim_{x\to 0}[-xT \ln(x)/\dot{m} + xC] \propto -\lim_{x\to 0} x \ln(x). \tag{5}$$

Application of l'Hôpital's rule to the limit (5) indicates that the limit is zero, so there is no way to obtain an infinite objective in the classical problem. The relativistic limit has a similar result. Thus, the globally optimal solution will not have an infinitesimal final spacecraft mass.

2.1.2. Can we deduce an upper limit on J?

By making a number of reasonable conjectures, a likely upper limit can be found for J. The upper limit on m_f is clearly the initial mass of 1500 kg. For a given heliocentric energy of the spacecraft orbit at impact, the absolute value of the dot product of the velocities $\vec{U}_{rel}$ and $\vec{v}_{ast}$ is maximised when the spacecraft impacts the asteroid in a retrograde fashion when both the spacecraft and the asteroid are at periapsis. Since it is unlikely that the spacecraft will exceed parabolic energy, the parabolic impact scenario can be used to ascertain a likely upper limit on J. The periapsis speeds of the spacecraft in this scenario and asteroid are 30.71 and 24.50 km/s, respectively. Thus, a likely upper limit on J is 2,029,328 MJ.

2.1.3. Bounding of the search space

Let us first examine how we will limit the rough global search to a sensible, yet still very large, portion of the solution space. It is clear that the cost function will be increased by (1) increasing the final spacecraft mass, (2) increasing the arrival v_∞, (3) arriving with a $\vec{v}_\infty$ that is more collinear with the velocity of the asteroid, or (4) arriving when the asteroid's speed is larger. The first factor indicates that the trajectory should employ gravity assists *in lieu* of thrust wherever possible.

The second, third and fourth factors indicate that the spacecraft should, if possible, be on a retrograde orbit and impact the asteroid when both the spacecraft and the asteroid are at or near periapsis. Thus, the trajectory should employ some sequence of gravity assists at the two gas giants at our disposal.

The first question is how to reach the gas giants. Given the very low departure v_∞ of 2.5 km/s, to avoid excessive thrusting, it is likely best to use Venus (V) and Earth (E) as the first and second gravity assist bodies, respectively, although an initial post-launch sequence of VVE may be more beneficial due to the large turning of the v_∞ vector needed at Venus. Based on prior work [5], it was evident that it should be possible to reach Jupiter with very little thrusting, since the cited work shows ballistic trajectories to Jupiter with launch v_∞ values of 3 km/s and even slightly less. The second question is what sequence of flybys to use at Jupiter and Saturn. Given their long periods and the flight time limit of 30 years, only a handful of combinations are practical.

Taking the above two questions into account, and given the short time available for obtaining an answer, we examined the following sequences of gravity assist bodies for the whole launch window. The planets are represented by their initial letter, with M being for Mars and A for the asteroid:

EVEEJSA	EVEEESA	EVEEJVESA
EVEEJSJA	EVEEEJSA	EVEEJVESJA
EVEESJA	EVEEESJA	EVEMJJA
EVEMEJSJA	EVEEEJSJA	EVEMJSA
EVEMEMJSJA	EVEEJESJA	EVEMJSJA

The paths with inner-solar-system flybys after flybys at Jupiter were examined for the outside chance that the increased v_∞ afforded upon return to the gas giants would be helpful.

This list of paths is by no means exhaustive; indeed, Section 4 will show that two other paths offer better performance. As a side note, if there were no flight time limit, or only a very large one, the gravity-assist combinations and the trajectory as a whole would take on a very different character.

2.2. Searching in the search space

With the software STOUR-LTGA, described fully in [2,3], automated grid searches for trajectories were made for each of the above paths, using low thrust only on the Earth to Venus leg. In STOUR-LTGA, low-thrust arcs are computed extremely quickly using a shape-based approach, where the shape is taken as the exponential sinusoid. To compensate for the likely non-optimality of following the given shape, a slightly higher thrust acceleration than that actually available is permitted, and a slightly higher launch v_∞ is permitted as well. Other constraints are also relaxed a little, to compensate for the roughness of the search. The grid search is over launch date and over launch v_∞ values. The ballistic legs of the trajectory are computed exhaustively [7], that is, all possible ballistic trajectories satisfying the relaxed constraints are computed, with the exception that resonant transfers were excluded due to time constraints (transfers where two sequential flybys are made of the same body separated by an integral number of body revolutions). For the low-thrust leg, a judicious selection, based on various criteria, is made to obtain a finite number of trajectories from the continuum of solutions available. Each of the selected solutions for the low-thrust leg is passed on to the exhaustive ballistic computation engine. For some paths, when a ten-day step size in the launch date and two launch v_∞ values were used, up to 30,000 trajectories were found.

Of the hundreds of thousands of trajectories found in total using STOUR-LTGA, a handful were selected on the basis of very high arrival v_∞ (on the order of 50 km/s), or of very high cost function. These promising solutions were then handed over to the local optimisation program, named MALTO.

2.3. Local optimisation

The local optimisation program, MALTO, is based on the algorithm formulated by Sims and Flanagan [4]. In this formulation, the low-thrust arcs are modelled as a series of impulsive velocity increments (ΔVs), and the flybys are modelled as instantaneous turns of the v_∞ vector. Each leg (i.e. from one flyby body or control point to the next one in time) is split into a number of segments, as shown in Fig. 1. Targeting is done by means of a match point, which occurs after a specified number of segments from the first control point. The trajectory is propagated forward in time from the first control point to the match point, and backwards in time from the next control point to the match point. Trajectory propagation is conic, except that at the temporal midpoint of the segments a discontinuity in the velocity (ΔV) is allowed. The maximum magnitude of the ΔV is equal to the available thrust acceleration multiplied by the duration of the segment. From the rocket equation, the mass drop corresponding to the ΔV is computed. When a sufficient number of segments is used (for near-circular orbits, 20 to 30 segments per revolution is normally sufficient), this formulation provides

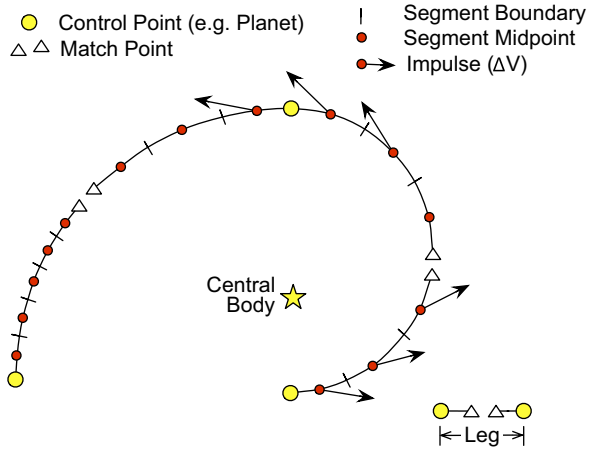

Fig. 1. Trajectory modelling in local optimiser, MALTO (after Sims and Flanagan [4]).

an excellent approximation to an actual low-thrust arc. Other constraints, such as flyby altitude constraints, are applied as needed.

The optimisation variables are the magnitude and direction of the impulses; the launch, flyby and arrival times; the incoming and outgoing v_∞ vectors at the flyby bodies; the outgoing/incoming v_∞ vectors at the launch/arrival body; and also the initial spacecraft mass (for the outside chance that the benefit of increased thrust acceleration could outweigh the penalty of reduced mass; initial mass would be reduced by dumping some propellant instantaneously). The optimisation engine used is SNOPT [8], which is based on the sequential quadratic programming method. SNOPT finds locally optimal solutions which satisfy the non-linear constraints. Appropriate scaling is used for the variables and analytic derivatives are used.

While the replacement of the low-thrust arcs with a series of impulsive ΔVs is a reasonable approximation, the question arises of how to obtain a smoothly varying state for the spacecraft which adequately represents the motion the spacecraft would have under low thrust. The approach taken here is simple. Essentially, a weighted average state is computed for intermediate times on any given segment. The known spacecraft state at the start of the segment is propagated forward conically up to the end time of the segment, and the known spacecraft state at the end of the segment is propagated conically backwards up to the start time of the segment. At any interior time point on the segment, a linearly weighted average is taken of the states at that time point as taken from the forward-propagated state history and the backwards-propagated state history. The direction of the thrust vector is taken as inertially fixed for the duration of the segment and equal to the direction of the impulsive ΔV on that segment. The magnitude of the thrust is taken as that magnitude which yields a characteristic velocity (from the rocket equation) equal to the impulsive ΔV. For the trajectory reported in Section 3, this procedure yields energy errors of less than 1 part in 10^5.

3. Competition results

The rough, global grid search using STOUR-LTGA yielded several hundreds of thousands trajectories. As a visual example, for the EVEEJSA path, the objective function is plotted versus the launch date in Fig. 2, which excludes thousands of trajectories with objective values below the range displayed.

Of the several trajectories optimised based on the best candidates from the rough global search, the best trajectory, designated trajectory A, used a path of EVEEEJSJA. Details are shown in Table 1 and Figs. 3 and 4. Thrusting occurs only on the EV leg. The long duration of the leg is suggestive that the addition of one or more flybys, immediately after Earth launch, may improve performance. The middle part of the trajectory, the triple-Earth flyby, is a very efficient way to reach Jupiter with a high flyby-v_∞. The heliocentric energy is shown as a function of time in Fig. 7. The best-performing trajectories had JSJA as the final part of the path, although trajectories ending in JSA were almost as good. The final Jupiter flyby in the JSJA path typically involved a very distant flyby, indicating that only limited use can be made of Jupiter for trajectories with geometry similar to trajectory A.

4. Post-competition results

Two further trajectories are presented here, both of which improve by about 1.4% on the objective value found for trajectory A. The first of these, designated trajectory B, was computed based on the remarkable gravity-assist sequence found by the Deimos team for their trajectory which took second place in the competition. Starting with the flyby dates and v_∞s reported by Deimos for their trajectory, MALTO was used to look for neighbouring, possibly better, local maxima. A better one was indeed found and is detailed in Table 2 and Fig. 5. The heliocentric energy is shown as a function of time in Fig. 7.

A second post-competition trajectory, designated trajectory C, was found by slowly building up in MALTO a flyby sequence of EVVEEEEJSJA which appeared energetically attractive and amenable to benefiting

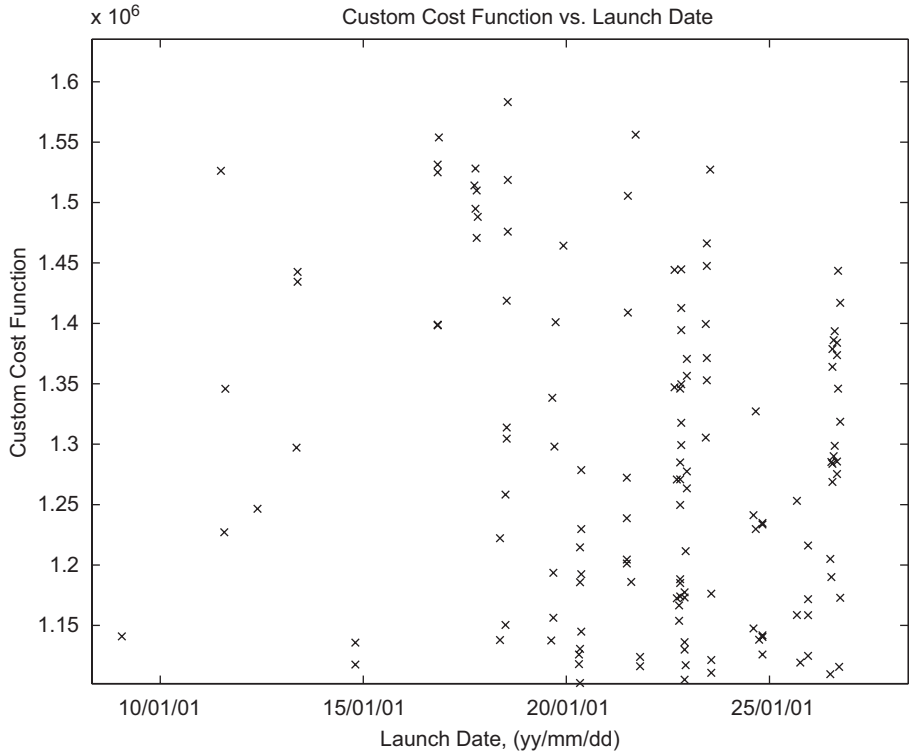

Fig. 2. Objective function versus launch date as computed in the broad search with STOUR-LTGA for the path EVEEJSA.

Table 1
Summary data for Trajectory A (EVEEEJSJA) which was ranked first in the competition with an objective function value of 1851322 MJ (the third-highest value in the present paper)

Body	Date (yyyy.mm.dd)	Days from launch	$\lvert\vec{v}_\infty\rvert$ (km/s)	Flyby radius (km)	S/c mass (kg)
Earth	2024.08.20	0.0	2.50	n/a	1500.0
Venus	2028.02.19	1278.0	7.04	6351	1442.9
Earth	2030.09.26	2228.0	11.86	10,132	1442.9
Earth	2033.12.28	3417.1	11.82	27,207	1442.9
Earth	2038.10.19	5172.8	11.87	6890	1442.9
Jupiter	2040.02.17	5659.0	14.41	1,216,508	1442.9
Saturn	2041.06.13	6141.5	15.30	90,909	1442.9
Jupiter	2050.06.01	9415.7	25.11	11,228,358	1442.9
2001 TW229	2051.11.26	9959.2	52.66	n/a	1442.9

handsomely from the classic v_∞-leveraging technique [9]. Trajectory details are shown in Table 3 and Fig. 6. The use of v_∞-leveraging is clearly evident in Fig. 6 where thrust against the velocity appears at apoapsis after each Earth flyby, and the resulting rise in the flyby v_∞ at the subsequent Earth flyby is evident in Table 3.

Trajectories A, B, and C, which all use almost identical final flybys of JSJ, are summarised in Table 4, and their energy-versus-time profiles are shown in Fig. 7. Trajectory C slightly outperforms trajectory B, which may be due in part to the less-meandering energy profile of trajectory C. Trajectory A has two flybys less than trajectory C which accounts for its somewhat poorer performance since propellant must be expended *in lieu* of the flybys. The start and end times, measured in days past launch, for each thrust arc of each trajectory are the

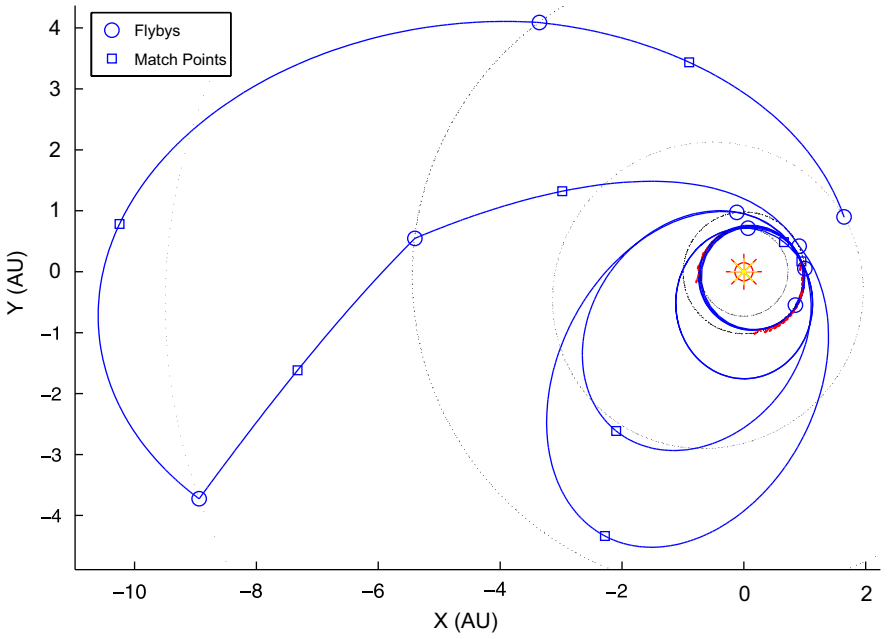

Fig. 3. Projection onto the J2000 ecliptic plane of trajectory A, having the path EVEEEJSJA.

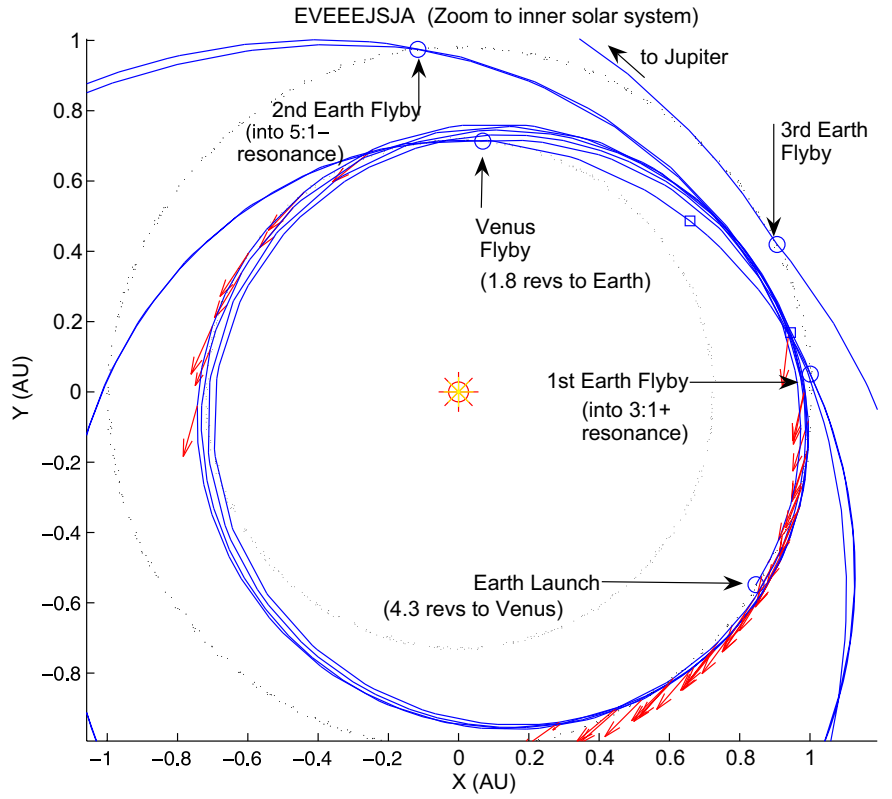

Fig. 4. Inner solar-system view of trajectory A (path EVEEEJSJA), projected onto the J2000 ecliptic plane.

Table 2
Summary data for trajectory B (EVVEEVVEVEJSJA) which has the second-highest objective found (1875689 MJ)

Body	Date (yyyy.mm.dd)	Days from launch	$\lvert\vec{v}_\infty\rvert$ (km/s)	Flyby radius (km)	S/c mass (kg)
Earth	2023.07.25	0.0	2.50	n/a	1500.0
Venus	2026.04.17	996.9	4.86	14,620	1489.3
Venus	2028.06.11	1782.6	4.81	12,305	1489.2
Earth	2029.03.04	2048.7	7.62	128,303	1489.2
Earth	2030.03.04	2414.0	7.62	11,314	1489.2
Venus	2031.03.10	2785.0	13.61	81,809	1489.2
Venus	2031.10.21	3009.7	13.62	6351	1489.0
Earth	2033.01.14	3460.2	14.03	16,236	1487.5
Venus	2035.12.26	4536.6	10.15	7866	1481.8
Earth	2038.12.11	5618.0	17.26	6678	1472.9
Jupiter	2040.02.28	6061.6	14.52	1,165,256	1461.7
Saturn	2041.06.23	6542.7	15.28	92,615	1461.7
Jupiter	2050.06.09	9815.2	25.08	11,309,174	1461.7
2001 TW229	2051.12.01	10,355.5	52.66	n/a	1461.7

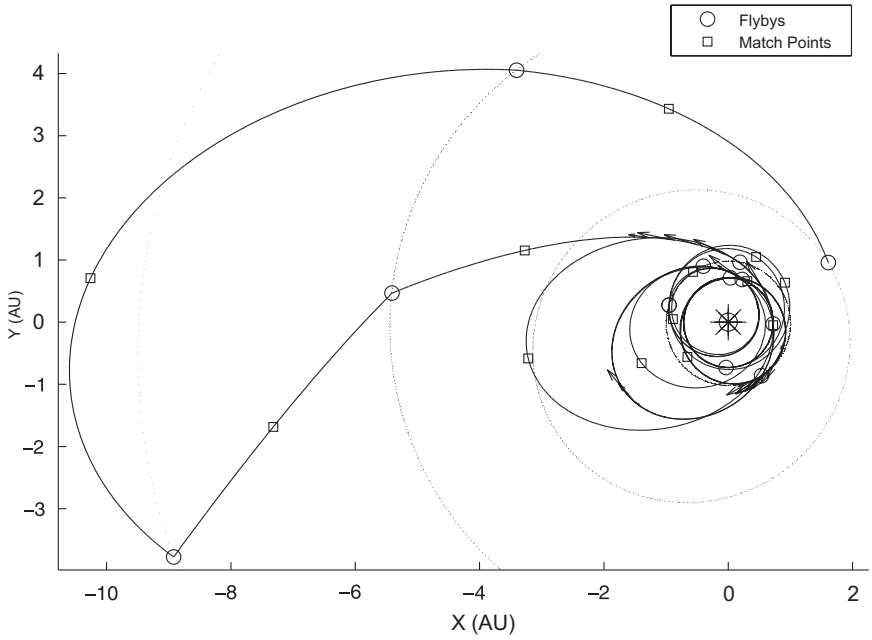

Fig. 5. Projection onto the J2000 ecliptic plane of trajectory B, having the path EVVEEVVEVEJSJA. This trajectory is based on the number-two ranked trajectory in the competition, found by the Deimos team.

following, where each pair of parentheses contains the start and end times for a single thrust arc. Trajectory A: (0, 1), (117, 170), (266, 320), (426, 455), (554, 628), (839, 927), (1118, 1225). Trajectory B: (0, 50), (266, 316), (1080, 1081), (2981, 2987), (3010, 3020), (3701, 3757), (4280, 4309), (5555, 5707). Trajectory C: (290, 297), (576, 597), (865, 892), (2360, 2400), (3224, 3286), (4608, 4708). As mentioned previously, all the thrust arcs for trajectory A occur before the first flyby. For trajectory B, thrust arcs appear on various legs and the final thrust arc straddles the final Earth flyby. Trajectory C also has thrusting on several legs, with no thrust applied after the final Earth flyby. In all cases, there is no thrust after the first Jupiter flyby, meaning that also on the final approach to the asteroid there is no thrust applied (which could perhaps be predicted from an analysis along the lines of Section 2.1.1).

Table 3
Summary data for trajectory C (EVVEEEEJSJA) which has the highest objective found (1877746 MJ)

Body	Date (yyyy.mm.dd)	Days from launch	$\lvert\vec{v}_\infty\rvert$ (km/s)	Flyby radius (km)	S/c mass (kg)
Earth	2023.07.08	0.0	2.50	n/a	1500.0
Venus	2026.04.06	1003.9	4.45	12,978	1492.1
Venus	2028.05.31	1789.4	4.43	13,464	1492.1
Earth	2029.01.11	2014.5	6.37	8134	1492.1
Earth	2031.01.05	2738.1	7.06	6678	1486.4
Earth	2033.11.30	3798.0	8.60	6678	1477.6
Earth	2038.10.20	5583.1	11.79	6678	1463.5
Jupiter	2040.02.17	6068.6	14.41	1,219,348	1463.5
Saturn	2041.06.14	6551.1	15.30	91,020	1463.5
Jupiter	2050.06.01	9825.8	25.10	11,288,649	1463.5
2001 TW229	2051.11.27	10,369.0	52.66	n/a	1463.5

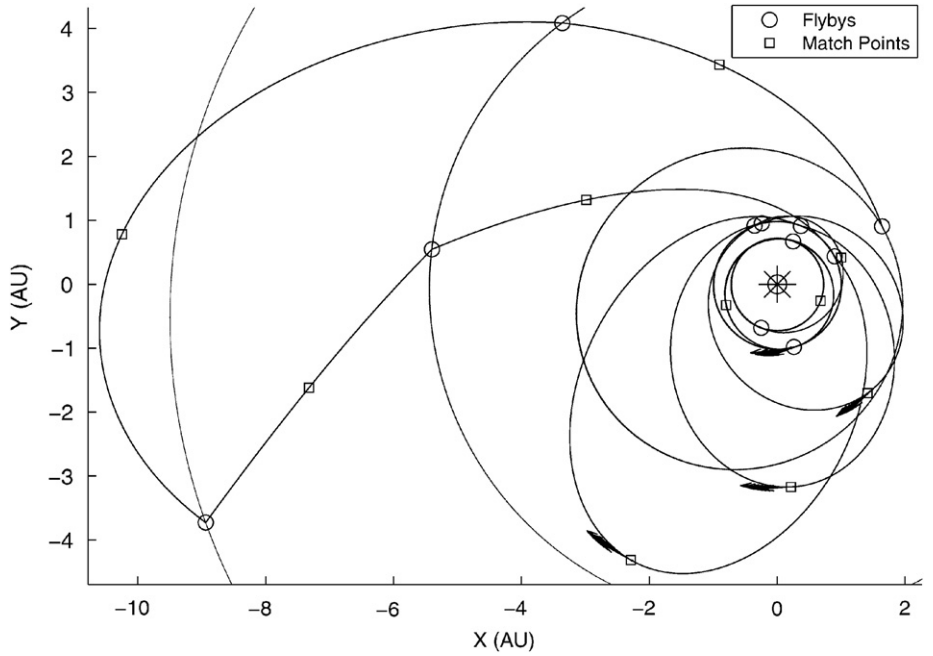

Fig. 6. Projection onto the J2000 ecliptic plane of trajectory C, having the path EVVEEEEJSJA.

Table 4
Comparison of trajectories A, B, and C

Traj.	Path	Impact date	Flight time (days)	Thrust duration (days)	Final mass (kg)	Objective function (MJ)
A	EVEEEJSJA	26 Nov 2051	9959.2	405	1442.9	1,851,322
B	EVVEEVVEVEJSJA	01 Dec 2051	10,355.5	271	1461.7	1,875,689
C	EVVEEEEJSJA	27 Nov 2051	10,369.0	259	1463.5	1,877,746

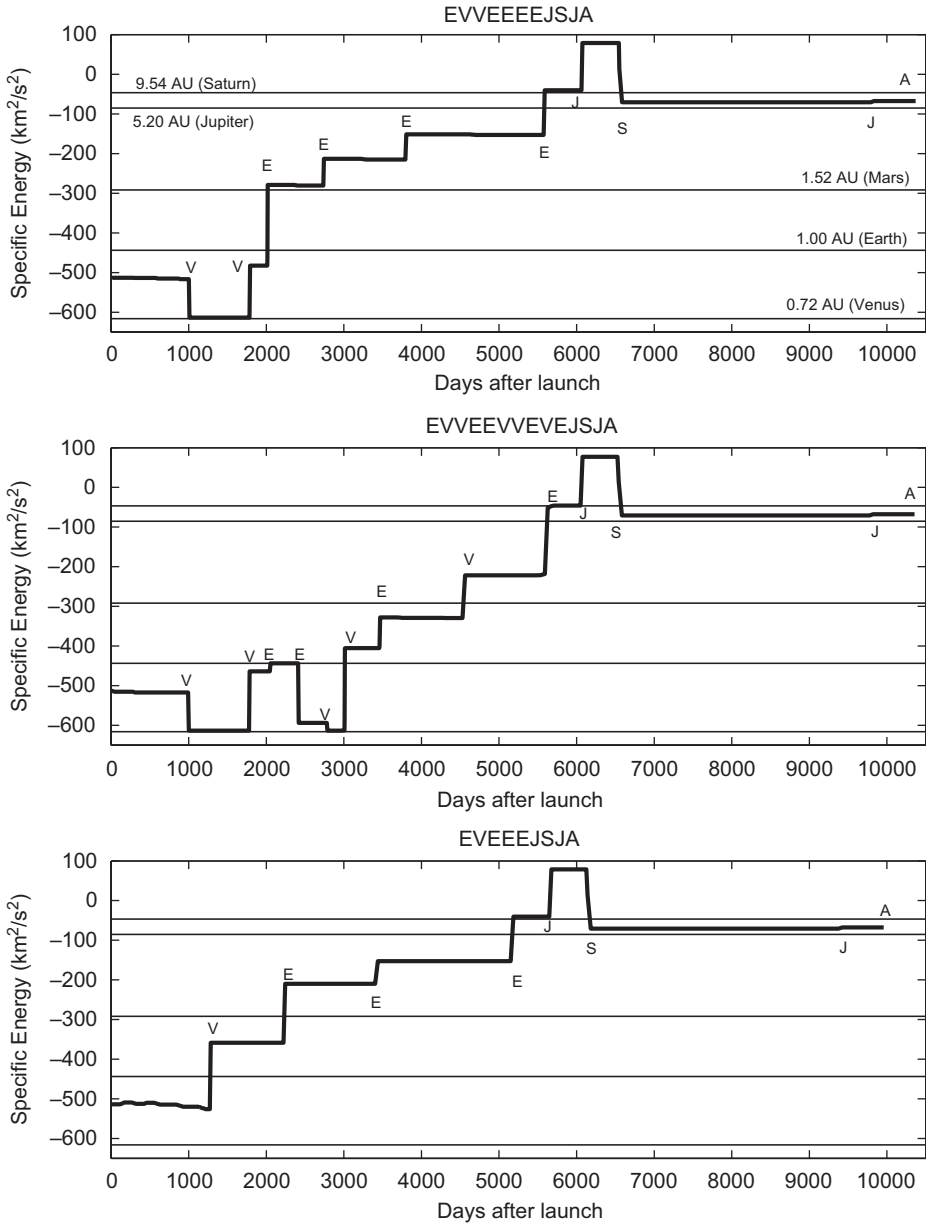

Fig. 7. Heliocentric specific energy of the spacecraft as a function of time for trajectories A, B, and C; flybys are indicated by the initial of the corresponding planet.

5. Conclusions

The mission design problem posed in the competition was certainly taxing of our current mission design methods. Two areas in particular stand out as being in need of improvement. The first is the rather simple idea of further automating the global search process, to free up the mission designer to concentrate on the physics of the problem. The second, and more important area, is that of what techniques to use in performing the global search. In the absence of robust and near-instantaneous local optimisation methods with large radii of convergence, it seems that a rough global search, based on simple numerical schemes coupled with mission design intuitions, is a necessary precursor activity to the local optimisation, and one which is a rich area for research.

Acknowledgements

This work was carried out at the Jet Propulsion Laboratory (JPL), California Institute of Technology, under a contract with the National Aeronautics and Space Administration (NASA). We would like to thank Ed Rinderle of JPL for expertly maintaining the MALTO software. We would also like to thank Ryan Russell, Try Lam, Powtawche Williams, Nathan Strange, Jennie Johannesen, Chen-Wan Yen, Carl Sauer, Seungwon Lee and Steven Williams, all of JPL, for their interest in the development of solutions for the competition. MALTO was developed at JPL (technical manager Jon Sims) under the auspices of the Low-Thrust Trajectory Tools task (managed by Larry Kos of NASA's Marshall Space Flight Center) within NASA's In-Space Propulsion Program. Lastly, we are indebted to the competition organisers for posing this stimulating intellectual challenge.

References

[1] D. Izzo, 1st ACT global trajectory optimisation competition: problem description and summary of the results, Acta Astronautica, this issue, doi:10.1016/j.actaastro.2007.03.003.

[2] A.E. Petropoulos, A shape-based approach to automated, low-thrust, gravity-assist trajectory design, Ph.D. Dissertation, Purdue University, W. Lafayette, IN, USA, 2001.

[3] A.E. Petropoulos, J.M. Longuski, Shape-based algorithm for automated design of low-thrust, gravity-assist trajectories, Journal of Spacecraft and Rockets 41 (5) (2004).

[4] J.A. Sims, S.N. Flanagan, Preliminary design of low-thrust interplanetary missions, AAS/AIAA Astrodynamics Specialist Conference, AAS Paper 99-338, Girdwood, Alaska, August 1999.

[5] A.E. Petropoulos, J.M. Longuski, E.P. Bonfiglio, Trajectories to Jupiter via gravity assists from Venus, Earth, and Mars, Journal of Spacecraft and Rockets 37 (6) (2000).

[6] T.T. McConaghy, T.J. Debban, A.E. Petropoulos, J.M. Longuski, Design and optimization of low-thrust trajectories with gravity assists, Journal of Spacecraft and Rockets 40 (3) (2003).

[7] S.N. Williams, Automated design of multiple encounter gravity-assist trajectories, M.S. Thesis, Purdue University, W. Lafayette, IN, USA, August 1990.

[8] SNOPT by P. Gill, W. Murray, M. Saunders, available from Stanford Business Software Inc. ⟨http://www.sbsi-sol-optimize.com/asp/sol_product_snopt.htm⟩.

[9] J.A. Sims, J.M. Longuski, A.J. Staugler, V_∞ leveraging for interplanetary missions: multiple-revolution orbit techniques, Journal of Guidance, Control, and Dynamics 20 (3) (1997) 10–20.